Received: 10 May 2017 | Revised: 17 March 2018 | Accepted: 19 May 2018
DOI: 10.1002/ett.3451

RESEARCH ARTICLE

WILEY

Scheduling and power adaptation for wireless local area networks with full-duplex capability

Rana A. Abdelaal | Ahmed M. Eltawil

The Henry Samueli School of Engineering, Department of Electrical Engineering and Computer Science University of California, Irvine, 4412 Engineering Hall Irvine, CA 92697, CA, USA

Correspondence
Rana A. Abdelaal, The Henry Samueli School of Engineering, Department of Electrical Engineering and Computer Science University of California, Irvine 4412 Engineering Hall Irvine, CA 92697 USA.
Email: rana@uci.edu

Abstract

In-band full-duplex communication has a great potential to enhance wireless local area networks, where full-duplex access points can support simultaneous uplink (UL) and downlink (DL) flows over the same frequency channel. This work presents a scheduling and power adaptation technique to manage interference in wireless local area networks with full-duplex capability. The proposed system focuses primarily on scheduling UL and DL clients that can be efficiently served simultaneously. First, we develop a DL client scheduling algorithm that allows for sum throughput gains with the existence of a UL client. Second, we manage the interference resulting from the UL flow via adjusting the UL transmit power to maximize rate for DL clients that are served in a multiuser multiple-input–multiple-output fashion.

1 | INTRODUCTION

In-band full-duplex (IBFD) is the ability to transmit and receive simultaneously in the same band through self-interference cancelation.[1,2] However, to take full advantage of IBFD, it is essential to manage the network interference cause by simultaneous transmission and reception. Managing interference due to IBFD has been studied in the existing literature. Recently, several publications[3-17] have considered the problem of self-interference cancelation in full-duplex (FD) systems by investigating different self-interference cancelation techniques to mitigate the self-interference signal. A combination of spatial isolation (propagation domain), analog, and digital cancelation techniques is typically used for IBFD.

Analog cancelation is necessary to obtain preliminary isolation to avoid radio frequency compression and saturation of the analog to digital converters.[3] Analog cancelation uses knowledge of the transmission to cancel self-interference in the RF signal before it is digitized. One approach to analog cancelation uses a second transmit chain to create an analog cancelation signal from a digital estimate of the self-interference.[4] Another approach is that the transmit signal is tapped at the transmit antenna feed, processed in the analog-circuit domain, and subtracted from the receive-antenna feed in order to cancel self-interference.[5] Jain et al[6] propose a design that utilizes a copy of the transmitted analog signal and uses a transformer in the analog domain to then create a perfectly inverted copy of the signal. The inverted signal is then connected to a circuit that adjusts the delay and attenuation of the inverted signal to match the self-interference that is being received on the receiver antenna from the transmitter antenna.

On the other hand, digital domain cancelation is based on the subtraction of the interference signal after the analog-to-digital converter.[8-11] Several experimental and analytical results show that the mitigation capability of digital cancelation techniques is highly dependent on the RF cancelation, mainly due to the transmitter and receiver radio circuits' impairments.[12-14]

*This work was partially supported by the National Science Foundation under Grant No. ECCS: 1710746

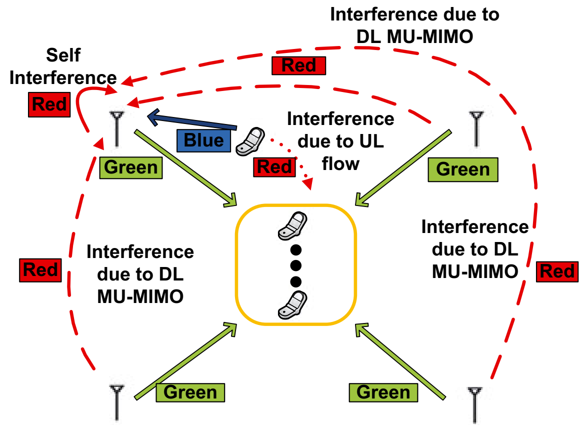

FIGURE 1 Interference in in-band full-duplex environment. DL, downlink; MU-MIMO, multiuser multiple-input multiple-output; UL, uplink

The self-interference signal could also be suppressed in the propagation domain. In propagation-domain suppression techniques,[7,15-17] the self-interference signal is suppressed before it is processed by the receiver circuitry. Propagation-domain self-interference suppression mitigates both the self-interference signal and the transmitter noise associated with it. In addition, mitigating the self-interference signal in the propagation domain decreases the effect of the receiver noise and increases the dynamic range allocated for the desired signal.

A common assumption made in the prior work is that the client that is being served on a downlink (DL) is also the client that is sending uplink (UL) packets to the access point (AP). Thus, the interference is purely self-interference. Network interference among clients will occur if different clients are considered for DL and UL, which may significantly deteriorate the throughput performance of IBFD wireless local area network (LANs). This is especially important in multiuser multiple-input–multiple-output (MU-MIMO) scenarios where an AP can send multiple frames to multiple clients at the same time over the same frequency resources.[18-21]

MU-MIMO has been considered in a number of wireless standards such as IEEE 802.11ac[22,23] and IEEE 802.11ax.[24,25] In MU-MIMO systems, each client can correctly decode packets simultaneously due to spatial diversity and precoding of channel weights by the transmitter. The total throughput, however, highly depends on the relationship between the channel responses and locations of scheduled clients.[22]

To illustrate the key challenges of MU-MIMO, IBFD network interference considers Figure 1, which shows the interference signals resulting from having simultaneous UL and DL flows. When the UL receiver and the DL transmitter are active at the same AP simultaneously, self-interference is generated (shown as the solid red arrow). However, when the UL AP is different than the DL AP, network interference is generated (shown as the dashed red arrows). The Figure assumes that one client is transmitting to one of the APs as a UL flow (shown as the solid blue arrow), and all the APs are transmitting to a set of DL clients, as DL flows (shown as the solid green arrows). The square in Figure 1 denotes the set of clients scheduled for DL MU-MIMO. In this case, the signal transmitted from the UL client can interfere with the DL clients. If the UL client is located close to the set of the DL clients, and the signal transmitted from the UL client is very strong, the DL clients will face high interference (shown as the dotted red arrow).

In order to mitigate the interference problem arising in such environment, a number of solutions have been proposed.[26-35] Those solutions capture additional transmission opportunities created by FD by modifying contention and backoff mechanisms. Goyal et al[26] develop a centralized MAC protocol to support asymmetric data traffic where network nodes may transmit data packets of different lengths, and they propose to mitigate the hidden node problem by employing a busy tone. To overcome this hidden node problem, the authors propose to adapt the 802.11 MAC protocol with the request-to-send (RTS)/clear-to-send (CTS) handshake. Choi et al[34] study the power allocation for IBFD system where clients operate in the half-duplex (HD) mode but the AP communicates by using the FD mode. In the aforementioned work,[34] the system model considers a single AP and multiple clients. The UL station (STA) is chosen randomly, then a DL STA with low interference from the UL STA and high received power from the AP is selected. Afterwards, a power control algorithm is used such that the DL signal-to-interference-plus-noise ratio (SINR) and UL SINR satisfy a threshold.[34]

A scheduling approach was studied for FD wireless networks in the work of Sahai et al,[35] such that the AP has a predetermined DL client and it aims at scheduling another UL client simultaneously. The AP randomly picks a UL client out of several ones that achieve a specific signal-to-interference (SIR) threshold at the DL client. A key shortcoming of the presented prior work is that any clients that achieve a specific SIR at the DL client is considered a good candidate.

Although, this type of optimization provides a guaranteed minimum throughput, it does not maximize the throughput. Moreover, in such schemes, finding a client that satisfies the SIR condition is done via exhaustive search over all the clients, which is time consuming.

This paper focuses on client scheduling at both the DL and the UL aiming at improving the sum rate in MU-MIMO wireless LANs with IBFD capability. The contributions of this paper can be summarized as follows:

- Proposed an efficient algorithm for client categorization based on received signal strength indicator;
- proposed a channel access mechanism for clients through contention window adjustment procedure, which results in scheduling a group of DL clients along with a UL client simultaneously with minimal interference;
- proposed a power adaptation algorithm, which adjusts the UL transmit power aiming at maximizing sum throughput of UL and DL clients.

The remainder of this paper is organized as follows. Section 2 presents the system model considered in this paper. In Section 3, we propose the scheduling technique that determines the UL and DL STAs to be served simultaneously. Section 4 presents the performance evaluation that confirms the effectiveness of the proposed algorithm. Finally, we conclude the paper in Section 5.

Notation. We use bold lower case for vectors, $\boldsymbol{a}$, whereas bold capital letters are used for matrices, $\boldsymbol{A}$. Furthermore, $||\boldsymbol{A}||$ stands for the norm of the matrix $\boldsymbol{A}$.

2 | SYSTEM MODEL

We consider an IBFD office wireless LAN scenario, in which APs are assumed to have FD capability. In other words, we consider that each AP can simultaneously transmit and receive. Throughout the paper, we will refer to the set of clients served on DL MU-MIMO as S_{DL}, whereas P_{UL} refers to the UL transmit power.

We assume that each client has n_s antennas, and each AP has n_a antennas. n_A refers to the number of APs that perform MU-MIMO multiplied by the number of antennas per AP. Channel gains are modeled according to *TGac* channel model D[25] and are assumed to be constant over the duration of each transmission. Since serving different clients results in interference in different directions, the proposed scheduling and power adaptation (SPA) technique plays an essential role in enhancing the system performance.

The received signal $\boldsymbol{y}_i^{dl} \in \mathbb{C}^{n_s}$ of the ith DL client is given by

$$\boldsymbol{y}_i^{dl} = \boldsymbol{H}_i \boldsymbol{x}_i^{dl} + \sum_{k=1,k\neq i}^{K} \boldsymbol{H}_i \boldsymbol{x}_k^{dl} + \boldsymbol{F}_{j,i} \boldsymbol{x}_j^{ul} + \boldsymbol{n}_i, \tag{1}$$

where

$$\boldsymbol{H}_i = \begin{bmatrix} \boldsymbol{H}_{1i} \\ \vdots \\ \boldsymbol{H}_{ai} \\ \vdots \\ \boldsymbol{H}_{Ai} \end{bmatrix}^T. \tag{2}$$

$\boldsymbol{H}_i$ is $n_s \times n_A$ matrix that represents the channel between the ith client and all APs. $\boldsymbol{H}_{ai}$ is $n_a \times n_s$ submatrix that represents the channel between the ath AP and the ith client, $\boldsymbol{x}_i^{dl} \in \mathbb{C}^{n_A}$ is the transmitted signal intended for the ith client from all APs. $\boldsymbol{x}_i^{dl} = \boldsymbol{w}_i^{dl} s_i^{dl}$, where $\boldsymbol{w}_i^{dl} \in \mathbb{C}^{n_A}$ is the MU-MIMO precoding vector for the transmitted signal intended to the ith receiver. In this paper we consider zero-forcing precoding. The transmit power is $||\boldsymbol{w}_i^{dl}||^2$, and s_i^{dl} is the transmitted symbol. The symbol power is $\boldsymbol{E}[|s_i^{dl}|^2] = \sigma^2_{s_i^{dl}}$, and we consider $\sigma^2_{s_i^{dl}}$ as unity.

Moreover, K is the number of coscheduled clients in DL MU-MIMO. $\boldsymbol{F}_{j,i}$ is $n_s \times n_s$ matrix that represents the interference channel from the UL client (served by the jth AP) to the DL client i due to the UL flow, and $\boldsymbol{x}_j^{ul} \in \mathbb{C}^{n_s}$ is the transmit signal of the UL client. $\boldsymbol{x}_j^{ul} = \boldsymbol{w}_j^{ul} s_j^{ul}$, where $\boldsymbol{w}_j^{ul} \in \mathbb{C}^{n_s}$ is the weighting vector in the UL direction, and the transmit power in the UL direction is $||\boldsymbol{w}_j^{ul}||^2$. s_j^{ul} is the data symbol in the UL direction, in which the transmitted symbol power is $\boldsymbol{E}[|s_j^{ul}|^2] = \sigma^2_{s_j^{ul}}$, and we consider $\sigma^2_{s_j^{ul}}$ as unity. Finally, $\boldsymbol{n}_i \in \mathbb{C}^{n_s}$ is the white Gaussian noise at the ith client with zero mean and variance equal to $\boldsymbol{E}[\boldsymbol{n}_i \boldsymbol{n}_i^H]$.

The received signal by the jth AP that is serving the UL client $\boldsymbol{y}_j^{ul} \in \mathbb{C}^{n_a}$ is given by

$$\boldsymbol{y}_j^{ul} = \boldsymbol{H}_{ju}\boldsymbol{x}_j^{ul} + \sum_{a=1, a\neq j}^{A} \sum_{k=1}^{K} \boldsymbol{G}_{a,j}\boldsymbol{x}_k^{dl} + \zeta_j + \boldsymbol{n}_j, \tag{3}$$

where

$$\zeta_j = \beta \sum_{k=1}^{K} \boldsymbol{G}_{j,j}\boldsymbol{x}_k^{dl}. \tag{4}$$

$\boldsymbol{H}_{ju}$ is $n_a \times n_s$ submatrix that represents the channel between the jth AP and the scheduled UL client, A is the number of APs, $\boldsymbol{G}_{a,j}$ is the $n_a \times n_a$ matrix that represents the channel between the ath AP and the jth AP, and $\boldsymbol{x}_k^{dl} \in \mathbb{C}^{n_a}$ is the transmit signal of the kth DL client. $\zeta_j \in \mathbb{C}^{n_a}$ is the self-interference, β is the self-interference cancelation coefficient, β represents a cancelation range of 70 to 90 dB in reference to the transmitter power, and $\boldsymbol{n}_j \in \mathbb{C}^{n_a}$ is the white Gaussian noise with zero mean and variance equal to $\boldsymbol{E}[\boldsymbol{n}_j\boldsymbol{n}_j^H]$.

The first term in (1) represents the intended signal, the second term represents the colayer interference, the third term represents the IBFD network interference, and the final term represents the additive noise. In (3), the first term is the intended signal in the UL direction, the second term is the interference resulting from serving the DL clients, the third term is the self-interference, and the final term is noise.

We define the SINR of a UL and DL flow as follows:

$$SINR^{ul} = \frac{\left|\boldsymbol{z}_j^H \boldsymbol{H}_{ju}\boldsymbol{w}_j^{ul}\right|^2}{\boldsymbol{z}_j^H \boldsymbol{R}_{Ij}\boldsymbol{z}_j} \tag{5}$$

$$SINR_i^{dl} = \frac{\left|\boldsymbol{z}_i^H \boldsymbol{H}_i\boldsymbol{w}_i^{dl}\right|^2}{\boldsymbol{z}_i^H \boldsymbol{R}_{Ii}\boldsymbol{z}_i}, \tag{6}$$

where $\boldsymbol{z}_j \in \mathbb{C}^{n_a}$ is the combining vector at the jth AP. Without loss of generality, we consider in this paper minimum mean-square-error combining vectors.[18] $\boldsymbol{R}_{Ij}$ is $n_a \times n_a$ interference plus noise covariance matrix at the AP serving the UL client, where $\boldsymbol{R}_{Ij} = \boldsymbol{E}[\boldsymbol{y}_j^{ul}\boldsymbol{y}_j^{ul^H}] - \boldsymbol{H}_{ju}\boldsymbol{w}_j^{ul}\boldsymbol{w}_j^{ul^H}\boldsymbol{H}_{ju}^H$.

Moreover, $\boldsymbol{z}_i \in \mathbb{C}^{n_s}$ is the combining vector for the ith receiver, and $\boldsymbol{R}_{Ii}$ is $n_s \times n_s$ interference plus noise covariance matrix at the ith receiver, where $\boldsymbol{R}_{Ii} = \boldsymbol{E}[\boldsymbol{y}_i^{dl}\boldsymbol{y}_j^{dl^H}] - \boldsymbol{H}_i\boldsymbol{w}_i^{dl}\boldsymbol{w}_j^{ul^H}\boldsymbol{H}_i^H$.

In addition, we define the total sum rate as follows:

$$R_{\text{tot}} = \log_2(1 + SINR^{ul}) + \sum_{i=1}^{K} \log_2(1 + SINR_i^{dl}). \tag{7}$$

The first and second terms denote the UL and DL rates, R_{ul} and R_{dl}, respectively.

3 | SPA: SCHEDULING AND POWER ADAPTATION

Traditionally, APs limit interference via frequency reuse or time division duplexing.[24] Theoretically, IBFD can be applied at each AP, and thus, an AP would support a UL and DL. However, viable IBFD choices will be limited due to the proximity of clients resulting in significant network interference. To solve the network interference problem, we propose that APs perform distributed MU-MIMO utilizing the aggregated bandwidth. Thus, the network serves multiple clients in the DL at a higher capacity via MU-MIMO, while supporting a UL link via IBFD. The main benefit of adopting this model is that there is a better chance of finding clients eligible for MU-MIMO IBFD since the physical space that all APs are covering is larger than each AP alone.

The following general system considerations are presented:

System Consideration 1: The selected UL client should be spatially separated from the DL clients to reduce cochannel interference.

System Consideration 2: DL clients should be spatially separated to maximize MU-MIMO DL rates.[18-20]

Figure 2 shows the importance of the system considerations discussed above. The y-axis represents the sum rate, where 4 APs are located on the vertices of a square with a side length of 10 m. A UL client is chosen randomly and is considered as a center of a circle where 4 DL clients are equally spaced on its circumference. By increasing the diameter of the circle,

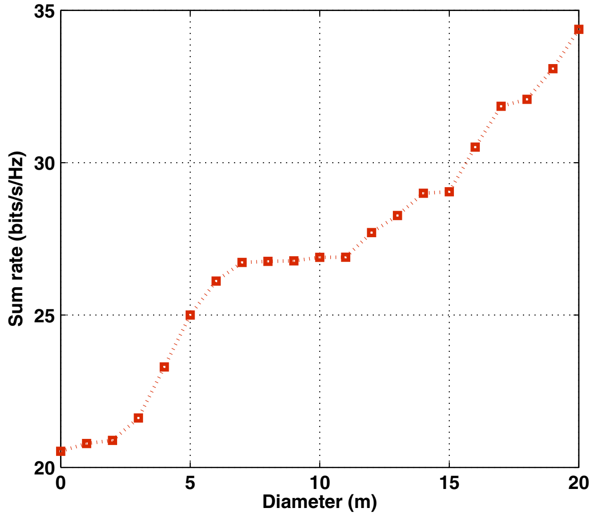

FIGURE 2 Sum rate with respect to the diameter of a circle with downlink clients on its circumference and an uplink client on its center

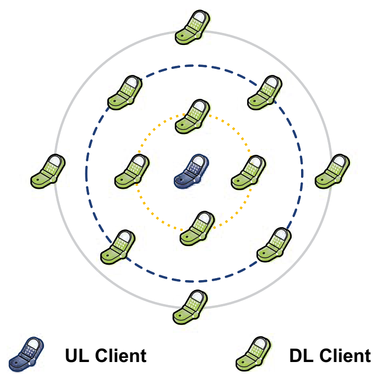

FIGURE 3 Example setup with downlink (DL) clients on circle's circumference and an uplink (UL) client on its center

the DL clients get further away from the UL client. Besides, the DL clients are separated from each other. An example for the setup is shown in Figure 3, where clients on the same circle are scheduled for DL simultaneously using MU-MIMO, whereas the client in the center of the circle is scheduled on the UL. In Figure 2, the sum rate is computed with respect to different circle diameter values. As shown, when the circle diameter is higher, ie, when the DL clients are far from the UL client and are far from each other, the interclient interference from the UL client is weak and the MU-MIMO gain is higher. Thus, the sum rate becomes high, as shown in Figure 3. On the other hand, a small circle diameter means a strong interclient interference from the UL client toward the DL clients and, also, DL clients are very close to each other, as a result, the sum rate is reduced.

3.1 | Client categorization

In order to categorize clients, we propose the use of controller unit (CU). One of the APs can act as the CU. The CU will be responsible for all aspects of MU operation. The CU will store sorted vectors of the received signal strength indicator (RSSI) indices of the APs as measured by the clients. For instance, a client with AP_a, AP_b, AP_c, AP_d has high RSSI from the ath AP, and low RSSI from the dth AP. The outcome of this process will be a lookup table with (A!) categories.

3.2 | Contention window adjustment procedure

The 802.11 protocol uses a carrier sense multiple access (CSMA) scheme, where the channel needs to be idle for any transmission or reception. When the channel is idle, a backoff timer is randomly chosen over the interval of $[0, CW]$, where CW stands for contention window size. In this paper, we propose CW adjustment mechanism, the proposed mechanism

TABLE 1 *CW* adjustment procedure

1: Initially, all clients have same $CW = CW_{int}$
2: After UL is selected, $CW = \alpha CW_{int}$, where $\alpha = \frac{1}{\boldsymbol{a}_i^u}$, $\boldsymbol{a}_i^u$ is the index of the UL AP within the client's sorted RSSI vector
3: If a client fails the rate condition, its *CW* is increased.
4: If a client passes the rate condition, the *CW* of other clients belonging to same category is increased.

Abbreviations: AP, access point; RSSI, received signal strength indicator; UL, uplink.

maintains backward compatibility. The legacy clients will still be able to demodulate and decode packet headers and backoff when the medium is busy.

Initially, a UL client is selected based on CSMA. This is by means of RTS and CTS signaling. Clients will transmit RTS to request to be scheduled in the UL, once a client receives the CTS signal intended for it, it will know that it is scheduled for UL transmission. Clients can attempt transmitting RTS at the same time, which causes collisions. In this case, clients will need to perform the backoff mechanism again.

Depending on the category (RSSI vector) of this UL client, it is better to schedule DL clients belonging to categories far from the UL client. In other words, to reduce interference with the UL client, it is better to schedule DL clients with RSSI vector with least significant digit equal to the most significant digit of the UL client, ie, if the UL client has AP_a, AP_b, AP_c, AP_d, DL clients is preferred to belong to the following: $(AP_d, AP_c, AP_b, AP_a), (AP_d, AP_b, AP_c, AP_a)$, $(AP_c, AP_d, AP_b, AP_a), (AP_c, AP_b, AP_d, AP_a), (AP_b, AP_d, AP_c, AP_a), (AP_b, AP_c, AP_d, AP_a)$.

Thus, using clients categorization, the (*CW*) size needs to be designed to control the backoff counters, such that clients belonging to the above categories get the smallest *CW* size. However, in some cases, based on the relative differences of signal strengths from APs, this potential client may not be a good candidate in terms of increasing the DL MU-MIMO rate benefits. Thus, the potential DL client will only be added to the set of scheduled DL clients S_{DL}, if the condition below is satisfied

$$R_{ul}^{p+1} + R_{dl}^{p+1} + R_{\text{potential}} \geq R_{ul}^{p} + R_{dl}^{p}, \tag{8}$$

where R_{dl}^{p} is the rate of the scheduled DL clients at the pth iteration, and the *CW* of all clients belonging to the same category will increase. However, if the rate condition is not satisfied, that client will solely increase its *CW*. The *CW* adjustment procedure is explained in Table 1, and the channel access mechanism is explained in the flow chart in Figure 4.

3.3 | Power adaptation

To improve performance, the UL power P_{UL} needs to be adjusted. Initially, the UL client uses full power. If the rate condition is not satisfied, P_{UL} is reduced, and the same steps are repeated. The process is repeated until reaching a minimum power $P_{\min}$ that satisfies a UL SINR threshold. The SPA algorithm is explained in Table 2. It is important to note that the selected P_{UL} is based on the rate; however, it is important to also consider throughput, which takes into account both rate and packets errors. Therefore, P_{UL} should be updated adaptively based on the throughput.

The first transmission/reception event for a set of clients will be based on the algorithm discussed in Table 2. However, upon completing each transmission/reception event, the status is checked. The goal is to use the results of every transmission/reception event (ie, packets are acknowledged or not) to increase or decrease P_{UL} accordingly. After each event, the throughput can be computed as follows:

$$T = (1 - PER_{UL}) * R_{UL} + (1 - PER_{DL}) * R_{DL}. \tag{9}$$

Then, the algorithm needs to decide whether to reduce or increase P_{UL}. The goal is to estimate T_l and T_h, which is the throughput at lower and higher P_{UL}, respectively. Then, the algorithm can select P_{UL} accordingly.

In order to estimate T_h and T_l prior to a transmission/reception event, the power adaptation algorithm is modified as explained below.

1. **Primary transmission/reception event:**
   When the link is established, use the primary P_{UL}^{p} selected by SPA algorithm in Table 2. Upon the completion of the event, use the number of packets that have been successfully received and the total number of packets transmitted to compute packet success ratio ($PSR = 1 - PER$). Then, compute the primary throughput T_p.

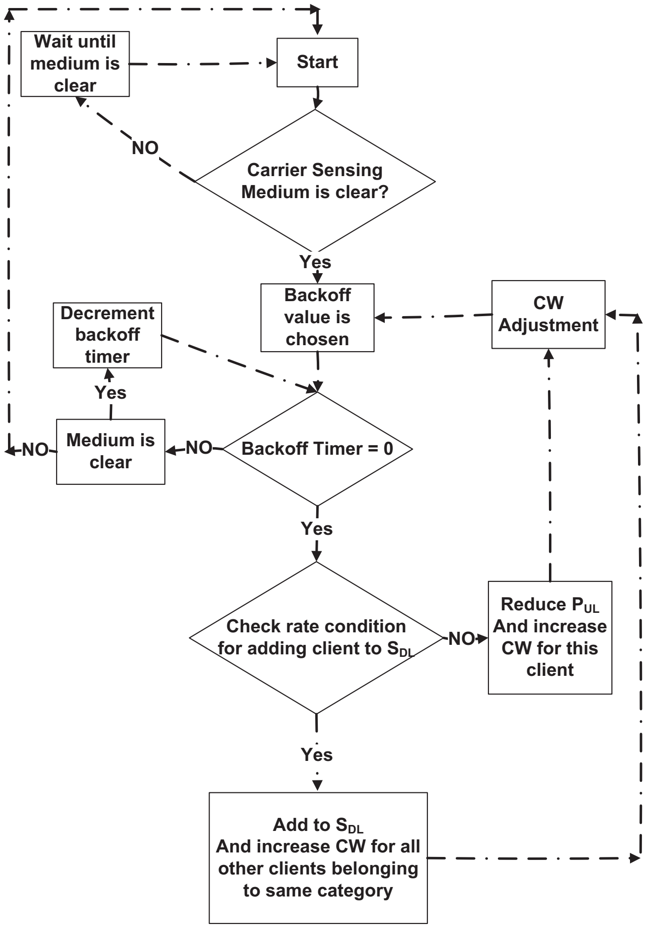

FIGURE 4 Channel access algorithm. CW, contention window

TABLE 2 Scheduling and power adaptation algorithm

1: Categorize clients based on sorted RSSI indices
2: UL client is selected
3: Update CW of clients based on the UL client and step 1
4: Initialize: $S_{DL} = 0$ and $P_{UL} = P_{\max}$
5: **while** $P_{UL} > P_{\min}$
6: **while** $\lvert S_{DL} \rvert < n_A$
7: Select a potential DL client
8: **if** $R_{ul}^{p+1} + R_{dl}^{p+1} + R_{\text{potential}} \geq R_{ul}^{p} + R_{dl}^{p}$
9: Add potential client and update S_{DL} accordingly
10: Increase CW of all clients belonging to the same category
11: Select a new potential client
12: **else**
13: Increase the contention window of this potential client
14: break from while loop
15: **end if**
16: **end while**
17: $P_{UL} = P_{UL} - \Delta$
18: **end while**

Abbreviations: CW, contention window; DL, downlink; RSSI, received signal strength indicator; UL, uplink.

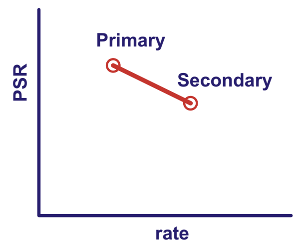

FIGURE 5 Primary and secondary information. PSR, packet success ratio

2. **Secondary transmission/reception event:**
   Calculate PER_{UL} and PER_{DL} and do the following: if $PER_{DL} > PER_{UL}$

$$P^s_{UL} = P^p_{UL} - \Delta, \tag{10}$$

else

$$P^s_{UL} = P^p_{UL} + \Delta. \tag{11}$$

Similar to step 1, compute the secondary throughput T_s, then the event that leads to higher throughput will be used as a current initial throughput T_c as follows:

$$T_c = \max(T_p, T_s). \tag{12}$$

P^c_{UL} is either the primary or the secondary P_{UL} based on the selection of T_c.

3. **Following events:**
   At this step, rate, PSR, and throughput for primary and secondary events have been computed. An example is shown in Figure 5. Note that P_{UL} affects throughput by affecting both rate and PSR. The effect on rate is known before transmission/reception. However, the effect on PSR is only known after the completion of the event. In this step, the target is to tune P_{UL} with a small tunable δ, such that

$$\begin{aligned} P^n_{UL} &= P^c_{UL} - \delta, \ \text{if} \ T_c < T_l \\ &= P^c_{UL} + \delta, \ \text{if} \ T_c < T_h, \end{aligned} \tag{13}$$

where P^n_{UL} is the new UL power.

In order to estimate T_l and T_h, we need to estimate $PSRs$ at both points. For that purpose, we use the primary and secondary points, as shown in Figure 5, and perform interpolation/extrapolation to find PSR_l and PSR_h. After doing so, we can get T_h and T_l and select the one that maximizes the throughput.

In summary, PSR is estimated at four points with updates upon each transmission/reception event according to the exponential moving average as follows:

$$PSR^n = \gamma PSR^{n-1} + (1-\gamma) * \frac{n_{\text{suc}}}{n_{\text{tot}}}, \tag{14}$$

where PSR^n is the new estimate, PSR^{n-1} is the previous estimate, $\gamma \in [0, 1]$ is the aging factor, n_{suc} is the number of successful packets, and n_{tot} is the total number of packets.

4 | PERFORMANCE EVALUATION

4.1 | Sample environment

To frame the discussion in a practical example, we adopt an office environment, as shown in Figure 6. In this scenario, the position of the APs is fixed, and clients are randomly distributed inside each cubicle. The main assumptions that we will follow throughout the paper are summarized in Table3.[36,37]

Our simulation follows the office environment described in Figure 6. In which, the office consists of four APs and comprises 64 cubicles. Each cubicle has four clients.[24]

We compare the performance of SPA with that of IBFD with power control that is presented in the work of Choi et al,[34] IBFD without power control, and HD conventional scenario. It is important to note that the aforementioned work[34] is only applicable for a single AP; thus, IBFD in the work of Choi et al[34] is implemented for each AP separately.

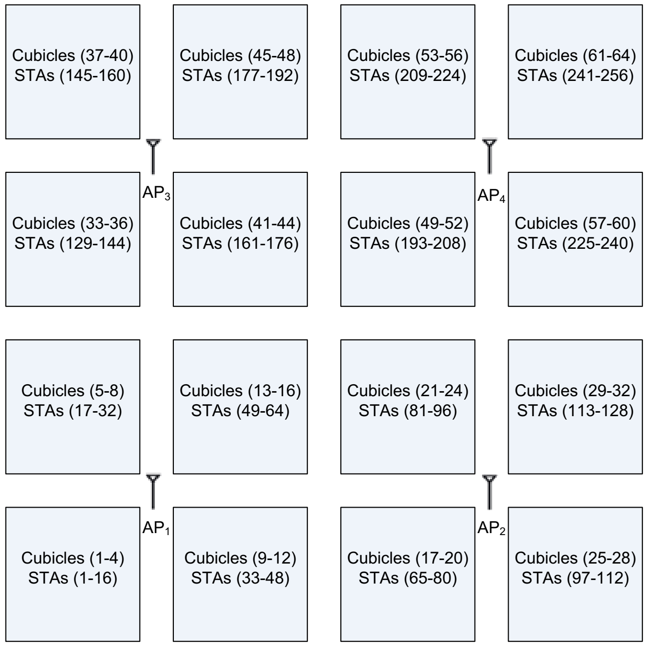

FIGURE 6 Office wireless local area networks scenario

TABLE 3 System parameters

Parameter	Value
Office area	20 m × 20 m
clients locations	randomly distributed within each cubicle
DL power	different across APs based on MU-MIMO
UL power	satisfy the lowest UL MCS Level 2
Frequency band	5 GHz
Channel bandwidth	80 MHz

Abbreviations: APs, access points; MCS, modulation coding scheme; MU-MIMO, multiuser multiple-input multiple-output; UL, uplink.

4.2 | Rate comparisons

Figure 7 shows the sum rate for different algorithms. The rate in the y-axis is a sum rate of coscheduled clients. As shown, the rate of IBFD without power control is worse than HD because the DL rate will be affected by high interference generated by the UL client. In contrast, the rate of IBFD system increases when power control is added. However, the high gains of IBFD cannot be achieved using the power control algorithm in the work of Choi et al.[34] As shown, HD and IBFD with power control[34] are close to each other, which is expected since network interference is limiting the benefits of IBFD. Thus, the power control algorithm in the aforementioned work[34] cannot utilize IBFD capability in the office scenario. This is due to the fact that choices are limited due to the proximity of clients, ie, the network interference caused by the UL will significantly reduce the SINR at the DL clients. However, SPA can overcome this problem because SPA has a better chance of finding clients that are eligible for IBFD, ie, SPA benefits from spatial separation. As shown, SPA algorithm outperforms all other algorithms by approximately 150%, 268%, and 101% with respect to HD, IBFD without power control, and IBFD with power control,[34] respectively. It is important to note that more than twice the rate is achieved by the SPA algorithm when compared with traditional HD due to the MU-MIMO gains.

4.3 | Fairness index

Figure 8 shows the fairness index for different IBFD algorithms. IBFD with SPA achieves comparable fairness index to the algorithm in work of Choi et al.[34] That is, the clients under SPA can be provided with fair scheduling opportunities. Note that SPA is adaptively assuring that UL and DL flows are achieving comparable good throughput.

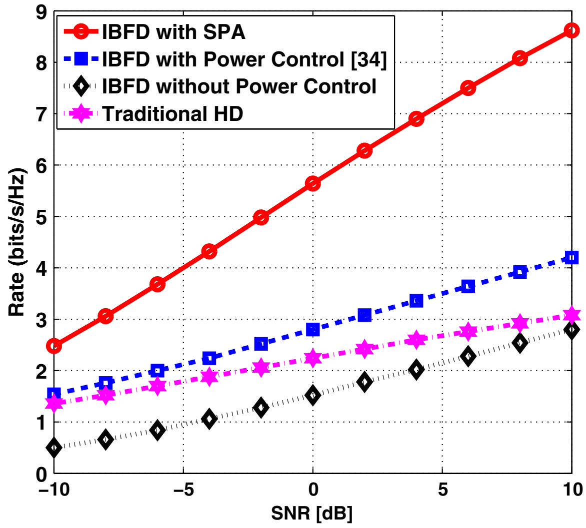

FIGURE 7 Rate comparison for office scenario. HD, half-duplex; IBFD, in-band full-duplex; SNR, signal-to-noise ratio

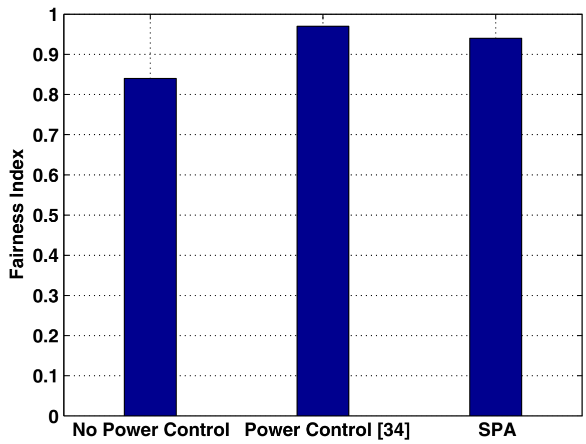

FIGURE 8 Fairness index comparison

4.4 | Impact of self-interference

In this paper, APs are equipped with elaborate antenna techniques and signal processing modules for self-interference cancelation. In previous simulations, we assumed perfect self-interference cancelation. Here, we show the impact of imperfect self-interference on different algorithms. Figure 9 shows the average SINR for UL and DL clients with respect to self-interference cancelation. The SINR of both UL and DL of IBFD increase as the self-interference cancelation increases since self-interference cancelation directly benefits the UL client and indirectly benefits the DL clients due to the power adaptation scheme. In addition, IBFD with power control in the work of Choi et al[34] can benefit from self-interference cancelation in both UL and DL directions. However, it cannot sufficiently overcome the problem caused by the proximity of clients resulting in significant network interference, and the SINR performance is then deteriorated. On the other hand, in the case of the IBFD without power control, UL SINR increases as self-interference cancelation increases, while DL-SINR does not change since the DL flow will suffer from the same interference regardless of self-interference cancelation. Figure 10 shows the difference between IBFD with SPA and IBFD in the aforementioned work[34] in terms of total sum rate. In the office scenario, IBFD in the aforementioned work[34] can serve up to 8 clients, on the other hand, IBFD with SPA can only serve up to 5 clients simultaneously. However, the sum rate of SPA exceeds the algorithm in aforementioned work,[34] as shown in Figure 10. Note that, in the aforementioned work,[34] the average interclient interference between clients increases because the distance between clients shorten; hence, the rate is degraded. Moreover, due to the distributed MU-MIMO model that is utilized in SPA, clients can get higher throughput opportunities.

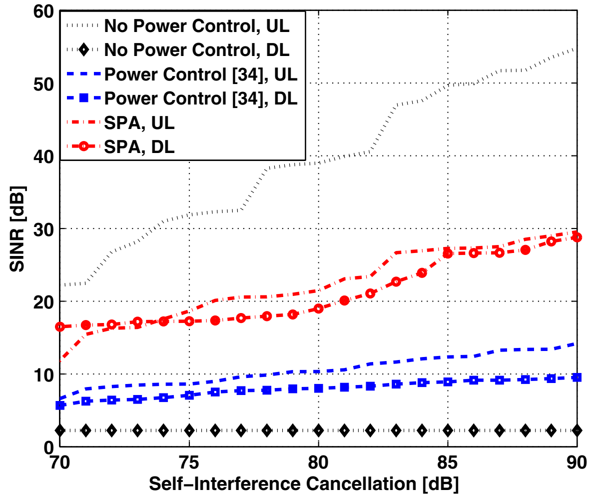

FIGURE 9 Signal-to-interference-plus-noise ratio (SINR) comparison for different self-interference cancelation. DL, downlink; SPA, scheduling and power adaptation; UL, uplink

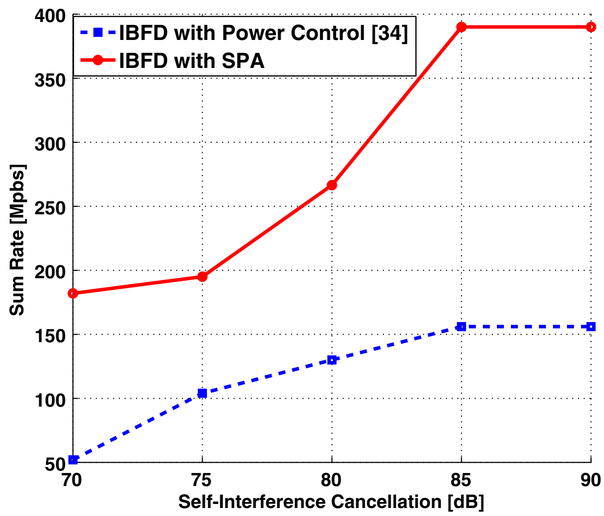

FIGURE 10 Sum rate comparison for different self-interference cancelation. IBFD, in-band full-duplex; SPA, scheduling and power adaptation

TABLE 4 Modulation coding scheme (MCS) levels of active links for in-band full-duplex

	SPA	Power Control[34]	No Power Control
MCS 7-8	38.28%	0.78%	48.59%
MCS 5-6	30.80%	0.79%	0.65%
MCS 3-4	30.60%	20.04%	0.48%
Lower	0.32%	78.39%	50.28%

4.5 | MCS levels comparison

Table 4 shows the modulation coding scheme (MCS) levels of active links. Active link is any scheduled DL or UL flow. Since SPA utilizes spatial separation, it provides high operation percentage on high MCS levels (7 and 8) that can be achieved approximately with 38.28%, 0.78%, and 48.59% using IBFD with SPA, with power control,[34] and without power control, respectively. The IBFD without power control achieves higher percentage than SPA because without power control, UL clients get high SINRs on the expense of DL clients getting very low SINRs. As can be noticed, SPA provides the lowest percentage of low MCS levels.

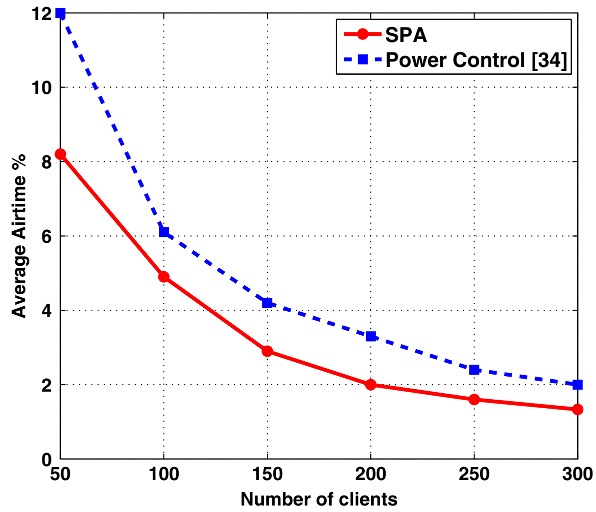

FIGURE 11 Average airtime for different number of clients. SPA, scheduling and power adaptation

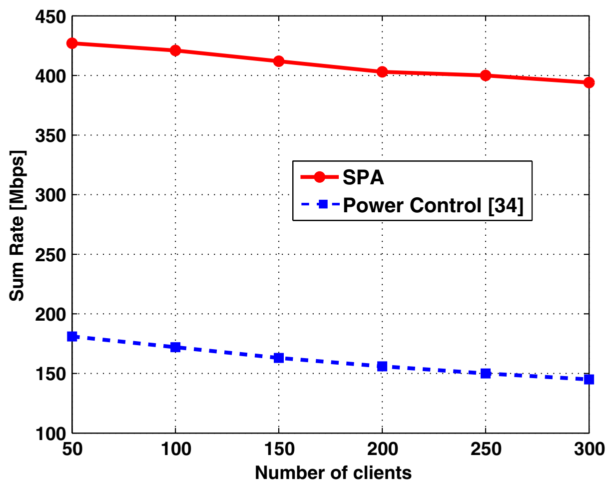

FIGURE 12 Average rate comparison for different number of clients. SPA, scheduling and power adaptation

4.6 | Number of clients

In this section, we show the effect of the number of clients on the average airtime and average rate. Figures 11 and 12 show the average airtime and average throughput with respect to the number of clients, respectively. It can be seen that the average airtime decreases with increasing the number of clients, and the algorithm presented in the work of Choi et al[34] has better airtime than SPA. However, as shown in Figure 12, SPA has better rate performance over the entire range of number of clients.

5 | CONCLUSIONS

In this paper, we present scheduling and power adaptation techniques to provide higher performance in the IBFD environment for office wireless LANs. Our proposed algorithm aims at selecting clients that can be efficiently served simultaneously with low interference between UL and DL transmissions. At a given time, a UL client is scheduled and its power is adapted while selecting multiple DL clients taking IBFD interference into account. Simulation results to evaluate system performance is presented, showing significant increase in rate compared to recent proposed scheduling and power control algorithms for IBFD.

ORCID

Rana A. Abdelaal http://orcid.org/0000-0002-6467-7622

REFERENCES

1. Ahmed E, Eltawil AM, Li Z, Cetiner BA. Full-duplex systems using multireconfigurable antennas. *IEEE Trans Wirel Commun*. 2015;14(11):5971-5983.
2. Sabharwal A, Schniter P, Guo D, et al. In-band full-duplex wireless: challenges and opportunities. *IEEE J Sel Areas Commun*. 2014;32(9):1637-1652.
3. Riihonen T, Wichman R. Analog and digital self-interference cancellation in full-duplex MIMO-OFDM transceivers with limited resolution in A/D conversion. Paper presented at: 2012 Conference Record of the Forty Sixth Asilomar Conference on Signals, Systems and Computers (ASILOMAR); 2012; Pacific Grove, CA.
4. Duarte M, Sabharwal A. Full-duplex wireless communications using off-the-shelf radios: feasibility and first results. Paper presented at: 2010 Conference Record of the Forty Fourth Asilomar Conference on Signals, Systems and Computers; 2010; Pacific Grove, CA.
5. Riihonen T, Werner S, Wichman R. Mitigation of loopback self-interference in full-duplex MIMO relays. *IEEE Trans Signal Process*. 2011;59(12):5983-5993.
6. Jain M, Choi JI, Kim T, et al. Practical, real-time, full duplex wireless. In: Proceedings of the 17th Annual International Conference on Mobile Computing and Networking (MobiCom); 2011; Las Vegas, NV.
7. Choi JI, Jain M, Srinivasan K, Levis P, Katti S. Achieving single channel, full duplex wireless communication. In: Proceedings of the Sixteenth Annual International Conference on Mobile Computing and Networking (MobiCom); 2010; Chicago, IL.
8. Ahmed E, Eltawil A. On phase noise suppression in full-duplex systems. *IEEE Trans Wirel Commun*. 2015;14(3):1237-1251.
9. Bharadia D, McMilin E, Katti S. Full duplex radios. *ACM SIGCOMM Comput Commun Rev*. 2013;43(4):375-386.
10. Duarte M, Dick C, Sabharwal A. Experiment-driven characterization of full-duplex wireless systems. *IEEE Trans Wirel Commun*. 2012;11(12):4296-4307.
11. Li N, Zhu W, Han H. Digital interference cancellation in single channel, full duplex wireless communication. Paper presented at: 2012 8th International Conference on Wireless Communications, Networking and Mobile Computing; 2012; Shanghai, China.
12. Ahmed E, Eltawil AM, Sabharwal A. Rate gain region and design tradeoffs for full-duplex wireless communications. *IEEE Trans Wirel Commun*. 2013;12(7):3556-3565.
13. Sahai A, Patel G, Dick C, Sabharwal A. On the impact of phase noise on active cancelation in wireless full-duplex. *IEEE Trans Veh Technol*. 2013;62(9):4494-4510.
14. Bliss DW, Hancock TM, Schniter P. Hardware phenomenological effects on cochannel full-duplex MIMO relay performance. Paper presented at: 2012 Conference Record of the Forty Sixth Asilomar Conference on Signals, Systems and Computers (ASILOMAR); 2012; Pacific Grove, CA.
15. Everett E, Duarte M, Dick C, Sabharwal A. Empowering full-duplex wireless communication by exploiting directional diversity. Paper presented at: 2011 Conference Record of the Forty Fifth Asilomar Conference on Signals, Systems and Computers (ASILOMAR); 2011; Pacific Grove, CA.
16. Everett E, Sahai A, Sabharwal A. Passive self-interference suppression for full-duplex infrastructure nodes. *IEEE Trans Wirel Commun*. 2014;13(2):680-694.
17. Duarte M, Sabharwal A, Aggarwal V, et al. Design and characterization of a full-duplex multiantenna system for WiFi networks. *IEEE Trans Veh Technol*. 2014;63(3):1160-1177.
18. Aryafar E, Anand N, Salonidis T, Knightly EW. Design and experimental evaluation of multi-user beamforming in wireless LANs. In: Proceedings of the Sixteenth Annual International Conference on Mobile Computing and Networking (MobiCom); 2010; Chicago, IL.
19. Shepard C, Yu H, Anand N, et al. Argos: Practical many-antenna base stations. In: Proceedings of the 18th Annual International Conference on Mobile Computing and Networking (MobiCom); 2012; Istanbul, Turkey.
20. Yang Q, Li X, Yao H, et al. BigStation: Enabling scalable real-time signal processing in large MU-MIMO systems. In: Proceedings of the ACM SIGCOMM 2013 Conference on SIGCOMM; 2013; Hong Kong, China.
21. Du Y, Aryafar E, Cui P, Camp J, Chiang M. SAMU: Design and implementation of selectivity-aware MU-MIMO for wideband WiFi. Paper presented at: 2015 12th Annual IEEE International Conference on Sensing, Communication, and Networking (SECON); 2015; Seattle, WA.
22. 802.11 WG IEEE802.11ac. Part 11: Wireless LAN medium access control (MAC) and physical layer (PHY) specifications: Enhancements for very high throughput for operation in bands below 6 GHz. Piscataway, NJ: IEEE Standards Association; 2013.
23. Ong EH, Kneckt J, Alanen O, et al. IEEE 802.11ac: Enhancements for very high throughput WLANs. Paper presented at: 2011 IEEE 22nd International Symposium on Personal, Indoor and Mobile Radio Communications; 2011; Toronto, Canada.
24. Stacey R. Specification framework for TGax. IEEE P802.11 Wireless LANs; 2016.
25. Merlin S. TGAx simulation scenarios. 11-14/0621 (Qualcomm); 2014.
26. Goyal S, Liu P, Gurbuz O, Erkip E, Panwar S. A distributed MAC protocol for full duplex radio. Paper presented at: 2013 Asilomar Conference on Signals, Systems and Computers; 2013; Pacific Grove, CA.

27. Singh N, Gunawardena D, Proutiere A, et al. Efficient and fair MAC for wireless networks with self-interference cancellation; Paper presented at: 2011 International Symposium of Modeling and Optimization of Mobile, Ad Hoc, and Wireless Networks; 2011; Princeton, NJ.
28. Tamaki K, Raptino HA, Sugiyama Y, et al. Full duplex media access control for wireless multi-hop networks; Paper presented at: 2013 IEEE 77th Vehicular Technology Conference (VTC Spring); 2013; Dresden, Germany.
29. Kim JY, Mashayekhi O, Qu H, Kazandjieva M, Levis P. Janus: A Novel MAC Protocol for Full Duplex Radio. Technical Report. Stanford, CA: Stanford University; 2013.
30. Zhou W, Srinivasan K, Sinha P. RCTC: Rapid concurrent transmission coordination in full duplex wireless networks. Paper presented at: 2013 21st IEEE International Conference on Network Protocols (ICNP); 2013; Goettingen, Germany.
31. Hossain E, Le LB, Niyato D. *Radio Resource Management in Multi-Tier Cellular Wireless Networks*. Hoboken, NJ; John Wiley & Sons; 2014.
32. Le LB, Lau V, Jorswieck E, et al. Enabling 5G mobile wireless technologies. *EURASIP J Wirel Commun Netw*. 2015;215(218).
33. Ramirez D, Aazhang B. Optimal routing and power allocation for wireless networks with imperfect full-duplex nodes. *IEEE Trans Wirel Commun*. 2013;12(9):4692-4704.
34. Choi W, Lim H, Sabharwal A. Power-controlled medium access control protocol for full-duplex WiFi networks. *IEEE Trans Wirel Commun*. 2015;14(7):3601-3613.
35. Sahai A, Patel G, Sabharwal A. Pushing the limits of full-duplex: design and real-time implementation. arXiv preprint arXiv 1107.0607; 2011.
36. IEEE 802.11-16/0024r1. Proposed TGax draft specification. IEEE 802.11 Wireless LANs; 2016.
37. IEEE 802.11-15/0132r16. Specification Framework Document. IEEE P802.11 Wireless LANs; 2015.

How to cite this article: Abdelaal RA, Eltawil AM. Scheduling and power adaptation for wireless local area networks with full-duplex capability. *Trans Emerging Tel Tech*. 2018;e3451. https://doi.org/10.1002/ett.3451